



Manuscript received 21 June 2023 Revised manuscript received 6 February 2024 Manuscript accepted 20 February 2024

Published online 1 March 2024

© 2024 The Authors. Gold Open Access: This paper is published under the terms of the CC-BY license.

Impact of rift history on the structural style of intracontinental rift-inversion orogens

Dylan A. Vasey^{1,2,*}, John B. Naliboff³, Eric Cowgill¹, Sascha Brune^{4,5}, Anne Glerum⁴, and Frank Zwaan^{4,6}

¹Department of Earth and Planetary Sciences, University of California, Davis, California 95616, USA

²Department of Earth and Climate Sciences, Tufts University, Medford, Massachusetts 02155, USA

³Department of Earth and Environmental Science, New Mexico Institute of Mining and Technology, Socorro, New Mexico 87801. USA

⁴GFZ German Research Centre for Geosciences, Telegrafenberg, 14473 Potsdam, Germany

⁵Institute of Geosciences, University of Potsdam, 14476 Potsdam-Golm, Germany

ABSTRACT

Although many collisional orogens form after subduction of oceanic lithosphere between two continents, some orogens result from strain localization within a continent via inversion of structures inherited from continental rifting. Intracontinental rift-inversion orogens exhibit a range of structural styles, but the underlying causes of such variability have not been extensively explored. We use numerical models of intracontinental rift inversion to investigate the impact of parameters including rift structure, rift duration, post-rift cooling, and convergence velocity on orogen structure. Our models reproduce the natural variability of rift-inversion orogens and can be categorized using three endmember styles: asymmetric underthrusting (AU), distributed thickening (DT), and localized polarity flip (PF). Inversion of narrow rifts tends to produce orogens with more localized deformation (styles AU and PF) than those resulting from wide rifts. However, multiple combinations of the parameters we investigated can produce the same structural style. Thus, our models indicate no unique relationship between orogenic structure and the conditions prior to and during inversion. Because the style of rift-inversion orogenesis is highly contingent upon the rift history prior to inversion, knowing the geologic history that preceded rift inversion is essential for translating orogenic structure into the processes that produced that structure.

INTRODUCTION

Plate-boundary collisional orogens form along boundaries between tectonic plates when two continental blocks collide following subduction of intervening oceanic lithosphere (e.g., Dewey and Bird, 1970). In contrast, intraplate orogens form within a continental plate by localization of strain along preexisting weaknesses (e.g., Vilotte et al., 1982; Ziegler et al., 1995; Raimondo et al., 2014). Some intraplate orogens reactivate weaknesses inherited from past collisions (e.g., the Tien Shan [Central Asia]; Jourdon et al., 2018), whereas others exploit weaknesses developed during continental rifting and thus are considered the result of rift inversion

Dylan A. Vasey **b** https://orcid.org/0000-0002

(Fig. 1; e.g., Cooper et al., 1989; Beauchamp et al., 1996; Marshak et al., 2000). A common presumption seems to be that the structural style of intracontinental rift-inversion orogens should be distinct from that of plate-boundary orogens, because during rift inversion, convergence is expected to occur by reactivation of extensional structures, resulting in distributed lithospheric thickening (e.g., Buiter et al., 2009; Vincent et al., 2016, 2018). However, many riftinversion orogens feature asymmetric underthrusting along lithosphere-scale shear zones and development of major fold-thrust systems (Fig. 1; e.g., Jammes et al., 2009), comparable to plate-boundary orogens (e.g., Willett et al., 1993; Beaumont et al., 1996).

Geodynamic numerical modeling of riftinversion orogenesis typically focuses on the High Atlas (Morocco) and the Pyrenees (Spain and France) (e.g., Buiter et al., 2009; Jammes et al., 2014; Dielforder et al., 2019; Jourdon et al., 2019; Wolf et al., 2021), though the structural styles of these orogens are distinct (Fig. 1). The High Atlas is broadly symmetric, flanked on both sides by fold-thrust belts of opposing vergence, and exhibits no underthrusting of one block of lithosphere beneath another (e.g., Beauchamp et al., 1999; Gomez et al., 2000). In contrast, the Pyrenees show asymmetric lithospheric underthrusting and fold-thrust belt development concentrated on one side of the orogen (e.g., Muñoz, 1992; Dielforder et al., 2019). The structure of these orogens varies considerably along-strike, and other rift-inversion orogens exhibit a range of symmetry and thrust-belt vergence (Fig. 1; e.g., the Greater Caucasus, Alice Springs [Australia], Araçuaí-West Congo [Brazil and Africa], Rocas Verdes [South America]; Philip et al., 1989; Fosdick et al., 2011; Raimondo et al., 2014; Fossen et al., 2020), but the controls on this variability are poorly understood.

We present two-dimensional (2-D) geodynamic numerical models designed to explore connections between the initial conditions of a rift prior to inversion and the structure of the resulting rift-inversion orogen. We find that changes in rift structure, rift duration, post-rift cooling, and convergence velocity dramatically change the large-scale structure of the resulting orogen, producing models that exhibit the distributed lithospheric thickening of the High Atlas, the asymmetric lithospheric underthrusting of the Pyrenees, and additional variability reminiscent of other natural rift-inversion orogens.

CITATION: Vasey, D.A., et al., 2024, Impact of rift history on the structural style of intracontinental rift-inversion orogens: Geology, v. 52, p. 429–434, https://doi.org/10.1130/G51489.1

⁶Department of Geosciences, University of Fribourg, 1700 Fribourg, Switzerland

^{*}Dylan.Vasey@tufts.edu

Rift-Inversion Orogens

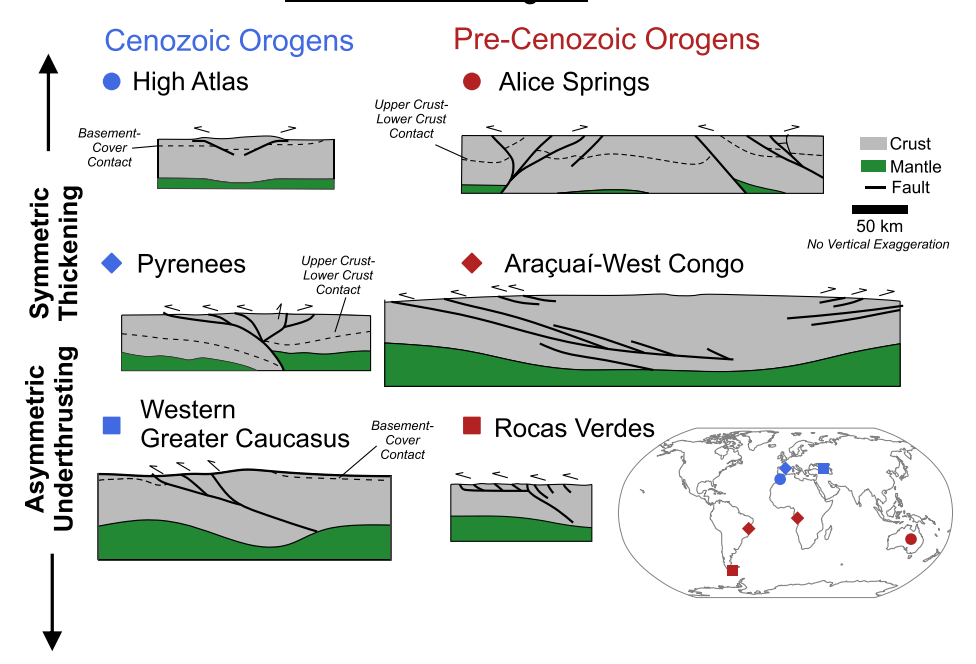


Figure 1. Schematic cross sections of Cenozoic and pre-Cenozoic rift-inversion orogens ordered by degree of symmetry (adapted from Philip et al., 1989; Beauchamp et al., 1999; Fosdick et al., 2011; Raimondo et al., 2014; Dielforder et al., 2019; Fossen et al., 2020). All orogens are shown in present-day configuration, except for Araçuaí-West Congo, which is shown at ca. 600–570 Ma.

GEODYNAMIC MODELING OF RIFT-INVERSION OROGENESIS

We modeled 2-D intracontinental rift inversion using the open-source, finite-element code ASPECT (Kronbichler et al., 2012; Heister et al., 2017; Naliboff et al., 2020; Bangerth et al., 2021; see the Supplemental Material¹ for detailed methods). To systematically compare the competing effects of rift structure, rift duration, post-rift cooling, and convergence rate, we performed 16 model simulations in a 1000×600 km model domain (Fig. 2A; Table 1). Each model began by using different combinations of lithospheric thickness and extension velocity to develop either a narrow or wide rift structure from an initial block of continental lithosphere (Fig. 2B, Table 1; e.g., Tetreault and Buiter, 2018). We stopped extension either at lithospheric breakup or at half the model time required to reach breakup. We inverted each of these four rifts with either no post-rift cooling phase or after a cooling period of 20 m.y. to get an initial sense of the effects of a post-rift cooling phase on orogenic style. For each of these eight models, we imposed two different convergence velocities during inversion (1 cm/yr, 5 cm/yr), with duration scaled

¹Supplemental Material. Methods, additional tables and figures, and videos of model runs. Please visit https://doi.org/10.1130/GEOL.S.25263154 to access the supplemental material; contact editing@geosociety.org with any questions.

(20 m.y., 4 m.y.) so that each orogen underwent the same amount of total convergence (200 km).

RESULTING STYLES OF RIFT-INVERSION OROGENESIS Style AU: Asymmetric Underthrusting

Several of our model rift-inversion orogens are characterized by asymmetric underthrusting of one block of lithosphere beneath another along a lithosphere-scale shear zone (style AU, Fig. 2C). This behavior is exemplified by model 1, formed from immediate inversion at 1 cm/yr of a narrow rift halfway to lithospheric breakup (Fig. 2A; Table 1). In this model, initial symmetric uplift of both sides of the rift gives way to localization of most strain along a left-dipping shear zone to the right of the former rift axis (Fig. 2C). Near the end of the model run, deformation propagates both along a synthetic shear zone to the right of the main structure and along an antithetic backthrust to the left.

Style DT: Distributed Thickening

By contrast, a second group of models does not localize deformation along lithosphere-scale thrust shear zones but instead undergoes distributed thickening of the lithosphere due to inversion along former normal faults (style DT). Model 5 (Fig. 2C) demonstrates this deformational style and tracks the immediate inversion at 1 cm/yr of a wide rift that has extended half-way to lithospheric breakup (Fig. 2A; Table 1). Distributed deformation during rifting leaves an

 \sim 400-km-wide zone of primarily upper-crustal normal faults with no distinct rift axis. Compression during inversion leads to reactivation of these structures as reverse faults as the lower crust and mantle lithosphere buckle and fold.

Style PF: Localized Polarity Flip

In a third set of models, deformation is localized asymmetrically along lithosphere-scale shear zones, but the individual shear zones are short-lived and are crosscut as new shear zones of opposite polarity take over (style PF). An endmember case of this orogenic style is model 3 (Fig. 2C), which results from immediate inversion at 1 cm/yr of a narrow rift at full lithospheric breakup (Fig. 2A; Table 1). In this case, initial symmetric asthenospheric upwelling at the rift axis gives way to localized deformation along two right-dipping, lithosphere-scale shear zones that are then subsequently crosscut by left-dipping shear zones. The resulting orogen is largely symmetric with only a hint of right-directed vergence (Fig. 2C).

Intermediate Modes of Orogenic Style

Half of the model results can be classified as distinctly style AU, DT, or PF rift-inversion orogens, while the other half exhibit orogenesis that is intermediate in character (Fig. 3). Intermediate behavior generally results from increasing localization of deformation as inversion proceeds, with style DT leading to style PF (model 15) or style AU (models 6, 7, 8, and 14), and style PF leading to style AU (models 2 and 10). The exception to this trend is model 4, in which initial localization along a pair of left-and right-dipping shear zones (style PF) gives way to more distributed deformation (style DT).

CORRELATIONS BETWEEN INITIAL CONDITIONS AND STRUCTURAL STYLE

To visualize the relationship between the model parameters explored here and the resulting structural styles, we assign each model a place on a schematic ternary diagram with vertices representing styles AU, DT, and PF (Fig. 3). We additionally place each of the natural orogens presented in Figure 1 on this diagram based on the overall vergence of major structures in the final orogen. The configuration of each individual orogen is contingent on the specific ensemble of parameters that produced it. However, there are general patterns between individual parameters and our three endmember orogenic styles.

The greatest influence on orogenic style is exerted by the structure of the rift (Fig. 3). Rift-inversion orogens that start with a narrow rift tend to have more localized deformation along lithosphere-scale shear zones, resulting in pronounced asymmetric underthrusting (style AU) or flipping polarity (style PF). By contrast, inver-

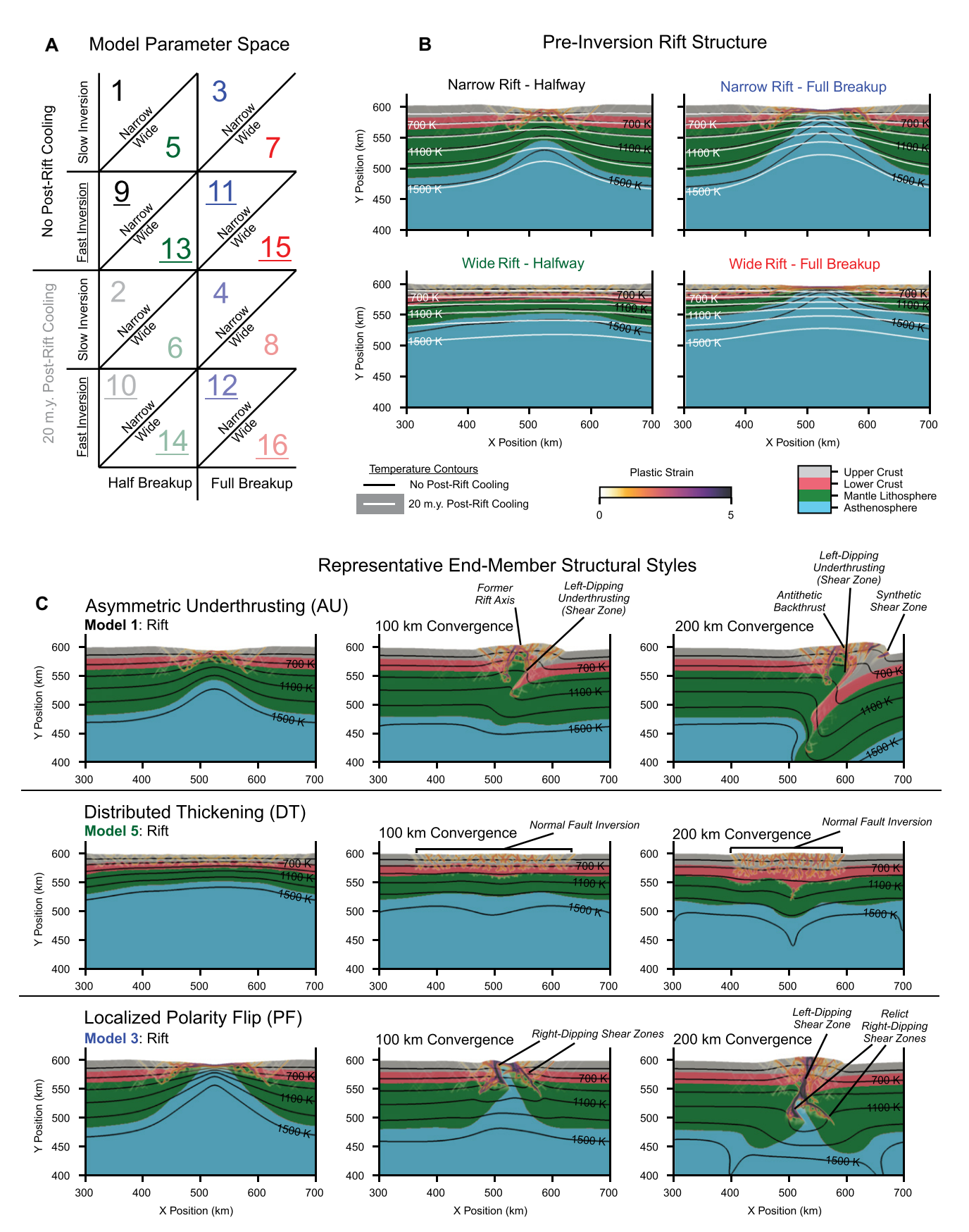


Figure 2. (A) Graphical overview of parameter space explored by the 16 models in this study. An initial narrow or wide rift is taken either half-way or all the way to lithospheric breakup. The resulting four rift structures (color-coded, see panel B) are inverted immediately (saturated colors) or after 20 m.y. of post-rift cooling (faded colors) at either a slower (1 cm/yr; no underline) or faster (5 cm/yr; underlined) convergence rate. (B) Initial conditions for the model orogens prior to inversion. (C) Rift inversion results exemplifying structural styles AU (asymmetric underthrusting), DT (distributed thickening), and PF (localized polarity flip), shown prior to inversion, after 100 km of convergence, and after 200 km of convergence.

TABLE 1. SUMMARY OF RIFT INVERSION MODEL PARAMETERS

| Model number | Model ID | Extension velocity (cm/yr) | Lithosphere thickness (km) | Rift duration | Post-rift cooling (m.y.) | Inversion velocity (cm/yr) | Inversion duration (m.y.) | Total model duration (m.y.) |
|-----------------|--------------|----------------------------------|----------------------------------|--------------------------|--------------------------------|----------------------------------|---------------------------------|-----------------------------------|
| 1 | 063022_rip_c | 0.5 | 120 | Halfway (16 m.y.) | 0 | 1 | 20 | 36 |
| 2 | 071822 rip b | 0.5 | 120 | Halfway (16 m.y.) | 20 | 1 | 20 | 56 |
| 3 | 070422_rip_e | 0.5 | 120 | Full breakup (32 m.y.) | 0 | 1 | 20 | 52 |
| 4 | 072022_rip_a | 0.5 | 120 | Full breakup (32 m.y.) | 20 | 1 | 20 | 72 |
| 5 | 070422_rip_c | 2 | 80 | Halfway (7.3 m.y.) | 0 | 1 | 20 | 27.3 |
| 6 | 071322_rip | 2 | 80 | Halfway (7.3 m.y.) | 20 | 1 | 20 | 47.3 |
| 7 | 070622_rip_a | 2 | 80 | Full breakup (14.5 m.y.) | 0 | 1 | 20 | 34.5 |
| 8 | 072022_rip_b | 2 | 80 | Full breakup (14.5 m.y.) | 20 | 1 | 20 | 54.5 |
| 9 | 080122_rip_a | 0.5 | 120 | Halfway (16 m.y.) | 0 | 5 | 3.4* | 19.4 |
| 10 | 080122_rip_e | 0.5 | 120 | Halfway (16 m.y.) | 20 | 5 | 3.5* | 39.5 |
| 11 | 080122_rip_b | 0.5 | 120 | Full breakup (32 m.y.) | 0 | 5 | 4 | 36 |
| 12 | 080122_rip_f | 0.5 | 120 | Full breakup (32 m.y.) | 20 | 5 | 4 | 56 |
| 13 | 080122_rip_c | 2 | 80 | Halfway (7.3 m.y.) | 0 | 5 | 4 | 11.3 |
| 14 | 080122 rip a | 2 | 80 | Halfway (7.3 m.y.) | 20 | 5 | 4 | 31.3 |
| 15 | 080122 rip d | 2 | 80 | Full breakup (14.5 m.y.) | 0 | 5 | 4 | 18.5 |
| 16 | 080122_rip_h | 2 | 80 | Full breakup (14.5 m.y.) | 20 | 5 | 4 | 38.5 |

*Models 9 and 10 failed to numerically converge prior to completion of the inversion stage and did not experience the full 200 km of inversion.

sion of a wide rift tends to result in orogens with more distributed thickening (style DT). However, this pattern does not hold across the full range of parameter space, with one orogen formed from a narrow rift (model 4) exhibiting elements of style DT and several orogens formed from wide rifts (models 6, 7, 8, 14, 15, and 16) displaying at least some element of styles AU or PF.

The influence of post-rift cooling and rift duration is less systematic. Rifting to full lithospheric breakup rather than halfway to breakup promotes localized deformation (styles AU and PF), though this is highly contingent on the rift structure (Fig. 3). Full breakup in a narrow rift tends to promote style PF over style AU (e.g., models 3 and 12), whereas inversion of a wide rift after full breakup promotes style AU over style DT (e.g., models 7, 8, and 16). Post-rift cooling promotes increasing localization of deformation (styles AU and PF). For inversion of narrow rifts (e.g., models 2, 10, and 12), the postrift cooling phase tends to result in shear zones of alternating polarity (style PF) rather than asymmetric underthrusting (style AU), whereas for inversion of wide rifts (e.g., models 6, 14, and 16), post-rift cooling tends to result in more distinctly asymmetric (style AU) behavior (Fig. 3).

The convergence velocity has less of an impact on the structure of the resulting orogen, but, in general, faster convergence velocities appear to promote asymmetric underthrusting (style AU). The most striking influence is seen by comparing models 3 (1 cm/yr) and 11 (5 cm/yr), which are equivalent in setup apart from convergence velocity. Model 3 is our exemplar orogen for style PF (Fig. 2C), whereas model 11 exhibits asymmetric underthrusting representative of style AU (Fig. 3).

COMPARISONS WITH PRIOR MODELING AND NATURAL EXAMPLES

Our study differs from prior work by exploring the range of structural variability in rift-inversion orogenesis as a general process (see the Supplemental Material for additional details). Studies focused on the Pyrenees tend to feature narrow rift structures taken close to lithospheric breakup with no post-rift cooling, resulting in orogens that resemble style AU (Jammes et al., 2014; Dielforder et al., 2019; Jourdon et al., 2019). Some modeling studies of continental collision include one or more riftinversion orogens for comparison with models with no pre-collisional extension, using parameters similar to the Pyrenees models that also yield style AU orogens (Jammes and Huismans, 2012; Wolf et al., 2021). One study that emphasizes the High Atlas includes wide rifts extended part way to lithospheric breakup with significant post-rift cooling, with resulting orogens exhibiting style DT (Buiter et al., 2009). By exploring a wider range of first-order variations in initial rift conditions, we capture both the AU orogenic style seen in models of the Pyrenees and the DT style seen in the Atlas-inspired model within a single suite of model results, in addition to other modes of deformation (style PF and intermediate modes) that do not resemble the High Atlas or Pyrenees (Fig. 3).

This initial exploration suggests that the path to developing a particular structural style is non-unique; different combinations of rift structure, rift duration, post-rift cooling, and/ or convergence velocity can result in the same first-order style (Fig. 3). Thus, in natural intracontinental rift-inversion orogens, the observed structural style may provide some indication of initial conditions but cannot uniquely pinpoint a single set of conditions. For example, the asymmetric underthrusting (style AU) observed in the Pyrenees or western Greater Caucasus (Fig. 1) could potentially be produced either by slower closure of a narrow rift immediately after partial lithospheric breakup (model 1) or by faster closure of a narrow rift extended to full lithospheric breakup (model 11).

Because the present-day structure of these orogens alone is insufficient to uniquely identify these parameters, using additional observations to constrain their geologic histories is critical.

Our study highlights the need to collect data that can differentiate between incremental tectonic histories in natural orogens. In particular, we note the importance of low-temperature thermochronology, which can provide constraints on both the timing and magnitude of deformation across major structures within collisional orogens (e.g., McQuarrie and Ehlers, 2017), as well as sedimentary records, which track changes in deposition and erosion as rifting and collision proceed (e.g., Tye et al., 2020). Future modeling studies that connect these first-order structural styles and their rift histories with patterns in thermochronology and/or sedimentary basin evolution will be essential for unraveling the complete history of intracontinental rift-inversion orogens.

CONCLUSIONS

Two-dimensional geodynamic numerical modeling of intracontinental rift inversion indicates that the structural style of rift-inversion orogens is highly dependent on initial conditions, including rift structure, rift duration, postrift cooling, and convergence velocity. Model orogens resulting from variations in these parameters can be classified using three structural styles: asymmetric underthrusting (AU), distributed thickening (DT), and localized polarity flip (PF). No systematic relationship exists between structural style and individual parameters, though narrow rifts, rifts that do not achieve lithospheric breakup, and rifts that cool prior to inversion tend to promote localized deformation (AU and PF) over distributed deformation (DT). These model results reconcile the range of structural styles seen in natural rift-inversion orogens but also indicate that a single structural style can be produced from multiple rift histories.

ACKNOWLEDGMENTS

This study was supported by U.S. National Science Foundation (NSF) grant 2050623 to E. Cowgill. ASPECT is hosted by the Computational Infrastructure for Geodynamics (CIG), supported by NSF grants 0949446 and 1550901. This work primarily used Extreme Science and Engineering Discovery

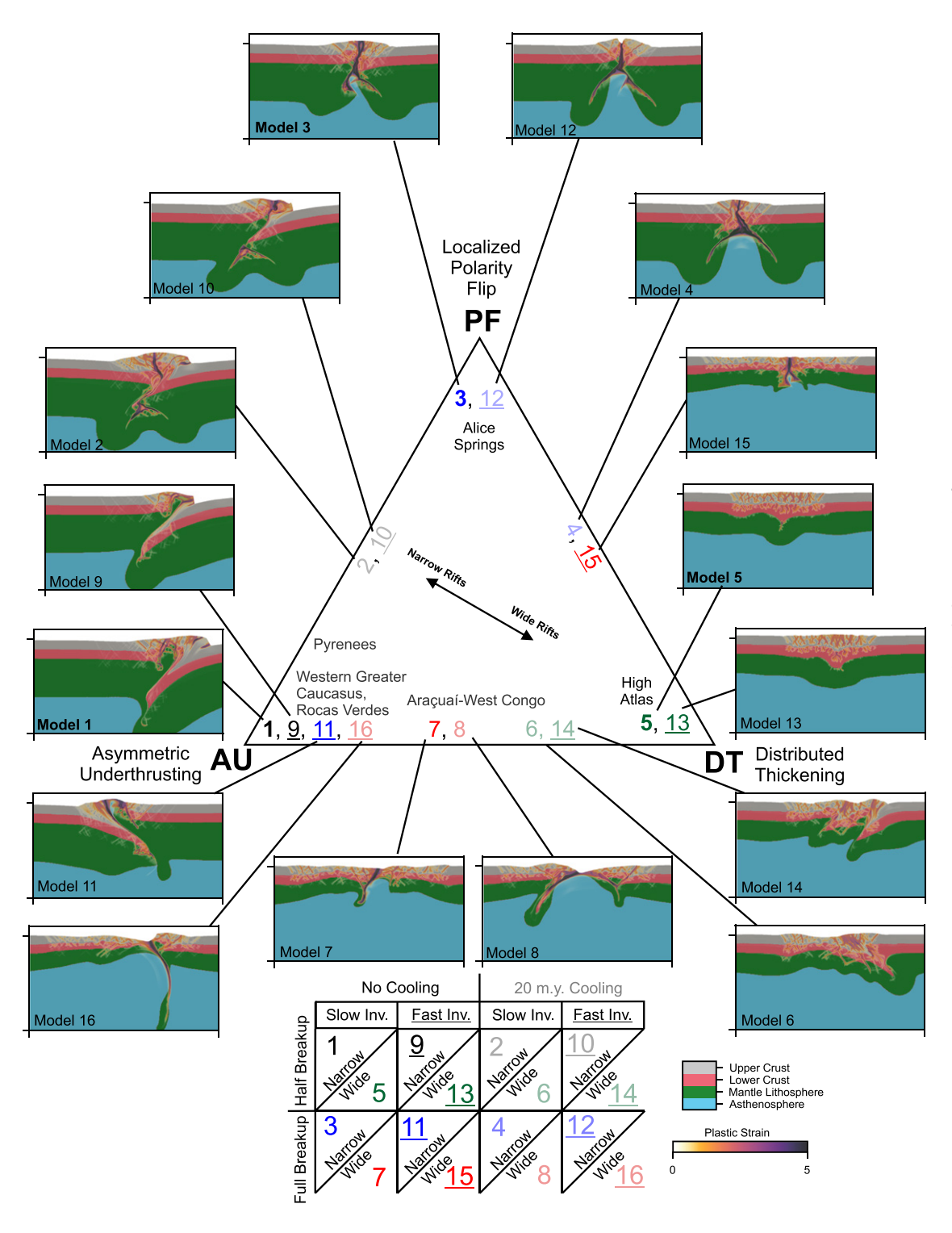


Figure 3. Schematic ternary diagram indicating the structural style of each model orogen. Model results are shown with the same model area as the panels in Figure 2. Doubleheaded arrow indicates that rift structure exhibits the strongest control on structural style. Natural examples of rift-inversion orogens are also plotted, showing a similar spread in structural style. Model number colors and underline style in the parameter space are as in Figure 2.

Environment (XSEDE) (Towns et al., 2014) allocations EES210024 (E. Cowgill) and EAR080022N (CIG) on Stampede2 (Texas Advanced Computing Center [TACC]), supported by NSF grant 1548562. Additional models were run using the Advanced Cyberinfrastructure Coordination Ecosystem: Services and Support (ACCESS) (Boerner et al., 2023) allocations EES230094 (D. Vasey) and TRA130003 (Tufts University, USA) on the Expanse cluster (San Diego Supercomputer Center at University of California San Diego), supported by NSF grants 2138259, 2138286, 2138307, 2137603, and 2138296. We thank L. Le Pourhiet and two anonymous reviewers for constructive reviews.

REFERENCES CITED

Bangerth, W., Dannberg, J., Fraters, M., Gassmoeller, R., Glerum, A., Heister, T., and Naliboff, J., 2021, ASPECT v2.3.0: Zenodo, https://doi.org/10.5281/ZENODO.5131909.

Beauchamp, W., Barazangi, M., Demnati, A., and Alji, M.E., 1996, Intracontinental rifting and inversion: Missour Basin and Atlas Mountains, Morocco: American Association of Petroleum Geologists Bulletin, v. 80, p. 1459–1481, https://doi.org/10.1306/64ED9A60-1724-11D7 -8645000102C1865D.

Beauchamp, W., Allmendinger, R.W., Barazangi, M., Demnati, A., Alji, M.E., and Dahmani, M., 1999, Inversion tectonics and the evolution of the High Atlas Mountains, Morocco, based on a geological-geophysical transect: Tectonics, v. 18, p. 163–184, https://doi.org/10.1029/1998TC900015.

Beaumont, C., Ellis, S., Hamilton, J., and Fullsack, P., 1996, Mechanical model for subduction-collision tectonics of Alpine-type compressional orogens: Geology, v. 24, p. 675–678, https://doi.org/10.1130/0091-7613(1996)024<0675:MMF-SCT>2.3.CO;2.

Boerner, T.J., Deems, S., Furlani, T.R., Knuth, S.L., and Towns, J., 2023, ACCESS: Advancing Innovation: NSF's Advanced Cyberinfrastructure Coordination Ecosystem: Services & Support,

- in Proceedings, Practice and Experience in Advanced Research Computing (PEARC) Conference, 23–27 July, 2023, Portland, Oregon: New York, Association for Computing Machinery, p. 173–176, https://doi.org/10.1145/3569951.3597559.
- Buiter, S.J.H., Pfiffner, O.A., and Beaumont, C., 2009, Inversion of extensional sedimentary basins: A numerical evaluation of the localisation of shortening: Earth and Planetary Science Letters, v. 288, p. 492–504, https://doi.org/10.1016 /j.epsl.2009.10.011.
- Cooper, M.A., Williams, G.D., de Graciansky, P.C., Murphy, R.W., Needham, T., de Paor, D., Stoneley, R., Todd, S.P., Turner, J.P., and Ziegler, P.A., 1989, Inversion tectonics—A discussion, in Cooper, M.A., Williams, G.D., eds., Inversion Tectonics: Geological Society, London, Special Publications, v. 44, p. 335–347, https://doi.org/10.1144 /GSL.SP.1989.044.01.18.
- Dewey, J.F., and Bird, J.M., 1970, Mountain belts and the new global tectonics: Journal of Geophysical Research, v. 75, p. 2625–2647, https://doi.org/10 .1029/JB075i014p02625.
- Dielforder, A., Frasca, G., Brune, S., and Ford, M., 2019, Formation of the Iberian-European convergent plate boundary fault and its effect on intraplate deformation in Central Europe: Geochemistry, Geophysics, Geosystems, v. 20, p. 2395–2417, https://doi.org/10.1029 /2018GC007840.
- Fosdick, J.C., Romans, B.W., Fildani, A., Bernhardt, A., Calderón, M., and Graham, S.A., 2011, Kinematic evolution of the Patagonian retroarc foldand-thrust belt and Magallanes foreland basin, Chile and Argentina, 51°30'S: Geological Society of America Bulletin, v. 123, p. 1679–1698, https://doi.org/10.1130/B30242.1.
- Fossen, H., Cavalcante, C., Konopásek, J., Meira, V.T., de Almeida, R.P., Hollanda, M.H.B.M., and Trompette, R., 2020, A critical discussion of the subduction-collision model for the Neoproterozoic Araçuaí-West Congo orogen: Precambrian Research, v. 343, https://doi.org/10.1016/j.precamres.2020.105715.
- Gomez, F., Beauchamp, W., and Barazangi, M., 2000, Role of the Atlas Mountains (northwest Africa) within the African-Eurasian plate-boundary zone: Geology, v. 28, p. 775–778, https://doi.org/10 .1130/0091-7613(2000)28<775:ROTAMN>2 .0.CO;2.
- Heister, T., Dannberg, J., Gassmöller, R., and Bangerth, W., 2017, High accuracy mantle convection simulation through modern numerical methods – II: Realistic models and problems: Geophysical Journal International, v. 210, p. 833– 851, https://doi.org/10.1093/gji/ggx195.
- Jammes, S., Manatschal, G., Lavier, L., and Masini, E., 2009, Tectonosedimentary evolution related to extreme crustal thinning ahead of a

- propagating ocean: Example of the western Pyrenees: Tectonics, v. 28, https://doi.org/10.1029/2008TC002406.
- Jammes, S., and Huismans, R.S., 2012, Structural styles of mountain building: Controls of lithospheric rheologic stratification and extensional inheritance: Journal of Geophysical Research: Solid Earth, v. 117, B10, https://doi.org/10.1029 /2012JB009376.
- Jammes, S., Huismans, R.S., and Muñoz, J.A., 2014, Lateral variation in structural style of mountain building: Controls of rheological and rift inheritance: Terra Nova, v. 26, p. 201–207, https://doi .org/10.1111/ter.12087.
- Jourdon, A., Le Pourhiet, L., Petit, C., and Rolland, Y., 2018, The deep structure and reactivation of the Kyrgyz Tien Shan: Modelling the past to better constrain the present: Tectonophysics, v. 746, p. 530–548, https://doi.org/10.1016/j.tecto.2017 .07.019.
- Jourdon, A., Le Pourhiet, L., Mouthereau, F., and Masini, E., 2019, Role of rift maturity on the architecture and shortening distribution in mountain belts: Earth and Planetary Science Letters, v. 512, p. 89–99, https://doi.org/10.1016/j.epsl .2019.01.057.
- Kronbichler, M., Heister, T., and Bangerth, W., 2012, High accuracy mantle convection simulation through modern numerical methods: Geophysical Journal International, v. 191, p. 12–29, https:// doi.org/10.1111/j.1365-246X.2012.05609.x.
- Marshak, S., Karlstrom, K., and Timmons, J.M., 2000, Inversion of Proterozoic extensional faults: An explanation for the pattern of Laramide and Ancestral Rockies intracratonic deformation, United States: Geology, v. 28, p. 735–738, https://doi.org/ 10.1130/0091-7613(2000)28<735:IOPEFA>2 0.CO:2.
- McQuarrie, N., and Ehlers, T.A., 2017, Techniques for understanding fold-and-thrust belt kinematics and thermal evolution, *in* Law, R.D., et al., eds., Linkages and Feedbacks in Orogenic Systems: Geological Society of America Memoir 213, p. 1–30, https://doi.org/10.1130/2017.1213(02).
- Muñoz, J.A., 1992, Evolution of a continental collision belt: ECORS-Pyrenees crustal balanced crosssection, in McClay, K.R. ed., Thrust Tectonics: Dordrecht, Springer, p. 235–246, https://doi.org /10.1007/978-94-011-3066-0_21.
- Naliboff, J.B., Glerum, A., Brune, S., Péron-Pinvidic, G., and Wrona, T., 2020, Development of 3-D rift heterogeneity through fault network evolution: Geophysical Research Letters, v. 47, e2019GL086611, https://doi.org/10.1029 /2019GL086611.
- Philip, H., Cisternas, A., Gvishiani, A., and Gorshkov, A., 1989, The Caucasus: An actual example of the initial stages of continental collision: Tectonophysics, v. 161, p. 1–21, https://doi.org/10.1016/0040-1951(89)90297-7.

- Raimondo, T., Hand, M., and Collins, W.J., 2014, Compressional intracontinental orogens: Ancient and modern perspectives: Earth-Science Reviews, v. 130, p. 128–153, https://doi.org/10.1016/j.earscirev.2013.11.009.
- Tetreault, J.L., and Buiter, S.J.H., 2018, The influence of extension rate and crustal rheology on the evolution of passive margins from rifting to break-up: Tectonophysics, v. 746, p. 155–172, https://doi.org/10.1016/j.tecto.2017.08.029.
- Towns, J., et al., 2014, XSEDE: Accelerating Scientific Discovery: Computing in Science & Engineering, v. 16, p. 62–74, https://doi.org/10.1109/MCSE.2014.80.
- Tye, A.R., Niemi, N.A., Safarov, R.T., Kadirov, F.A., and Babayev, G.R., 2020, Sedimentary response to a collision orogeny recorded in detrital zircon provenance of Greater Caucasus foreland basin sediments: Basin Research, v. 33, p. 933–967, https://doi.org/10.1111/bre.12499.
- Vilotte, J.P., Daignières, M., and Madariaga, R., 1982, Numerical modeling of intraplate deformation: Simple mechanical models of continental collision: Journal of Geophysical Research: Solid Earth, v. 87, p. 10,709–10,728, https://doi.org/10 .1029/JB087iB13p10709.
- Vincent, S.J., Braham, W., Lavrishchev, V.A., Maynard, J.R., and Harland, M., 2016, The formation and inversion of the western Greater Caucasus Basin and the uplift of the western Greater Caucasus: Implications for the wider Black Sea region: Tectonics, v. 35, p. 2948–2962, https://doi.org/10.1002/2016TC004204.
- Vincent, S.J., Saintot, A., Mosar, J., Okay, A.I., and Nikishin, A.M., 2018, Comment on "Relict basin closure and crustal shortening budgets during continental collision: An example from Caucasus sediment provenance" by Cowgill et al. (2016): Tectonics, v. 37, p. 1006–1016, https://doi.org/10 .1002/2017TC004515.
- Willett, S., Beaumont, C., and Fullsack, P., 1993, Mechanical model for the tectonics of doubly vergent compressional orogens: Geology, v. 21, p. 371–374, https://doi.org/10.1130/0091-7613(1993)021<0371:MMFTTO>2.3.CO;2.
- Wolf, S.G., Huismans, R.S., Muñoz, J.-A., Curry, M.E., and Beek, P. van der, 2021, Growth of collisional orogens from small and cold to large and hot—Inferences From geodynamic models: Journal of Geophysical Research: Solid Earth, v. 126, e2020JB021168, https://doi.org/10.1029 /2020JB021168.
- Ziegler, P.A., Cloetingh, S., and van Wees, J.-D., 1995, Dynamics of intra-plate compressional deformation: The Alpine foreland and other examples: Tectonophysics, v. 252, p. 7–59, https://doi.org/10.1016/0040-1951(95)00102-6.

Printed in the USA